POWER MEASUREMENT

Power measurement has a wide variety of applications. It is of importance primarily for the testing, monitoring, and maintenance of the energy supply network and of electrical equipment. It is also required in high-frequency and low-power circuits.

A wide variety of instruments and transducers are available for the measurement of power in ac and dc circuits. Analog instruments are available, but the recent trend has been toward digital instruments, because of their better performance and remote communication capabilities.

This article reviews the state and the trends of power measurement. The concept of electric power is first introduced; then common measurement methods and instruments adopted in different situations are discussed.

DEFINITION OF THE MEASURED QUANTITIES

Power can be defined as the time rate of energy transfer or energy dissipation in a load. It is dimensionally expressed as [J/s]. The electric power in a circuit, at any instant, equals the product of the current in the circuit and the voltage across its terminals at that instant. Dimensionally we have

$$[\mathrm{J/s}] = [\mathrm{J/C}][\mathrm{C/s}] = [\mathrm{V}][\mathrm{A}] = [\mathrm{W}] \tag{1}$$

Dc Circuits

In a dc circuit, if the voltage and current are constant, the electrical power P dissipated by a load (L) fed by a power supply (E) is the product of the voltage V_L across the load and the current I_L flowing in it:

$$P - V_\mathrm{L} I_\mathrm{L} \tag{2}$$

Ac Circuits

In the case of ac-fed circuits, the instantaneous rate of energy flow, or *instantaneous power,* is defined as the product of the instantaneous voltage drop across the load and the instantaneous current flowing through it:

$$p(t) = v(t)i(t) \tag{3}$$

It changes continuously, because of the cyclic variations in current and voltage. For this reason, its mean value over a defined time interval is generally considered.

Sinusoidal Circuits. The simplest case is that of a sinusoidal supply feeding a purely resistive load, where there is no phase difference between voltage $v(t)$ and current $i(t)$. The instantaneous power $p(t)$ is given by

$$p(t) = VI(1 - \cos 2\omega t) \tag{4}$$

in which V and I are the rms values of $v(t)$ and $i(t)$, respectively, and ω is the power supply angular frequency.

The instantaneous power is a unidirectional pulsating energy flow, given by a sum of two terms: a constant value VI, representing the average power, which gives the net energy transfer, and an oscillating component with a doubled angular frequency. In circuits fed by periodic ac voltages, it is then relevant to define the *average power* P dissipated in one period T (also called the *real* or *active power*):

$$P = \frac{1}{T}\int_0^T p(t)\,dt \tag{5}$$

In the case of purely reactive loads the phase difference between the voltage drop across the load and the current flowing through it is of 90°. The instantaneous power $p(t)$ is given by

$$p(t) = VI\cos 2\omega t \tag{6}$$

so there is no active power consumption in a reactive load. This is because energy is stored in the reactive load as electromagnetic or electrostatic energy for a certain time, and then returned to the power supply.

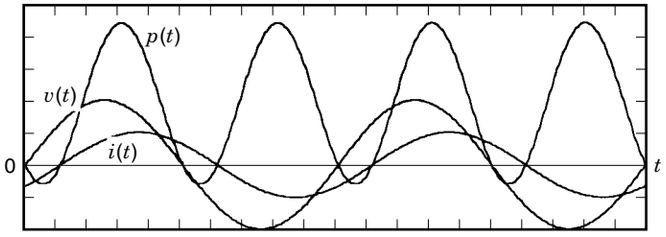

Figure 1. Waveforms of instantaneous power (p), voltage (v), and current (i).

In the case of a sinusoidal supply, the resistive and purely reactive loads can be expressed by a real or a pure imaginary number, respectively. Since the load generally is not a pure element, it can be represented by a complex quantity, the impedance value. In this situation, the waveforms of the voltage $v(t)$, current $i(t)$, and instantaneous power $p(t)$ are shown in Fig. 1. The load impedance can also be represented by an equivalent circuit, such as a pure resistance R_{EQ} and a pure reactance X_{EQ} in series (Fig. 2). In this case the electrical power dissipated in the load Z_{L} can be expressed as the sum of the two power components dissipated on the resistance and reactance of the equivalent circuit. Because there is no active power dissipation in the reactance X_{EQ}, the average power is as follows:

$$P = V_{\text{REQ}} I_{\text{L}} = V_{\text{L}} I_{\text{L}} \cos\phi \tag{7}$$

The factor cos ϕ appearing in Eq. (7) is referred as the *power factor,* because it yields the amount of power consumed as a fraction of $V_{\text{L}} I_{\text{L}}$. In fact, only a fraction of the voltage V_{L} contributes to the average power, because the component $V_{X\text{EQ}}$ (the drop across the reactance) does not produce any active power dissipation, as it is orthogonal to the current I_{L} flowing into the load (Fig. 2).

The quantity

$$Q = V_{X\text{EQ}} I_{\text{L}} = V_{\text{L}} I_{\text{L}} \sin\phi \tag{8}$$

—called, by analogy, the *reactive power*—is introduced as a consequence of the voltage drop across a pure reactance. It is a term with zero mean value, representing an energy oscillating equally in both directions, and therefore does not give any contribution to the active power.

The product of the load voltage and current rms values,

$$P_{\text{A}} = V_{\text{L}} I_{\text{L}} \tag{9}$$

—called the *apparent power*—is a figure of merit representing the maximum energy transfer capability of a system and used to express the power consumption of various electrical devices.

Both apparent power and reactive power are dimensionally homogeneous with power and thus might be expressed in watt. But they have a different nature. While relationships involving instantaneous power and real power satisfy the principle of conservation of energy, apparent power and reactive power do not satisfy any conservation principles. To stress the different physical meaning of P_{A} and Q, their units are called voltampere (VA) and reactive voltampere (var), respectively.

The relationship existing between apparent power, active power and reactive power is given by

$$P_{\text{A}} = \sqrt{P^2 + Q^2} \tag{10}$$

Nonsinusoidal Circuits. A case of great interest is that of the power measurement on distorted waveforms. As an example, advanced systems for electric power production in industrial applications are commonly based on solid-state power components. They have proved to be extremely effective and useful, but, unfortunately, the waveforms that these devices produce on the power line have characteristics far different from the sinusoidal waveforms.

In this case, obviously, the above symbolic representation can no longer be applied. In the general case of distortion of both voltage and current waveforms, we have

$$\begin{aligned} v(t) &= \sum_{h=0}^{M} V_h \sin h\omega t \\ &= V_0 + V_1 \sin\omega t + V_2 \sin 2\omega t + V_3 \sin 3\omega t + \cdots \\ i(t) &= \sum_{k=0}^{M} I_k \sin(k\omega t - \phi_k) \\ &= I_0 + I_1 \sin(\omega t - \phi_1) + I_2 \sin(2\omega t - \phi_2) \\ &\quad + I_3 \sin(3\omega t - \phi_3) + \cdots \end{aligned} \tag{11}$$

The active power, always defined as the mean power dissipated in one fundamental period, is then

$$\begin{aligned} P &= \frac{1}{T}\int_0^T \sum_{h=0}^{M} V_h \sin h\omega t \sum_{k=0}^{M} I_k \sin(k\omega t - \phi_k)\, dt \\ &= \frac{1}{T}\int_0^T \sum_{h=0}^{M}\sum_{k=0}^{M} V_h I_k \sin h\omega t \sin(k\omega t - \phi_k)\, dt \\ &= \frac{1}{T}\int_0^T \sum_{h=0}^{M}\sum_{k=0}^{M} V_h I_k \\ &\qquad \frac{\cos[(h-k)\omega t + \phi_k] - \cos[(h+k)\omega t - \phi_k]}{2}\, dt \\ &= V_0 I_0 + \sum_{h=1}^{M} V_h I_h \cos\Phi_h \\ &= V_0 I_0 + V_1 I_1 \cos\phi_1 + V_2 I_2 \cos\phi_2 + V_3 I_3 \cos\phi_3 + \cdots \end{aligned} \tag{12}$$

—that is, the sum of the active powers of the various frequency components contained in the voltage and current. As an example, voltage and current waveforms in both time and frequency domains are shown in Figs. 3 and 4, respectively. Voltage components of order 1 (fundamental), 3, 5, 7, and 9 and current components of order 1, 5, and 11 are present. In

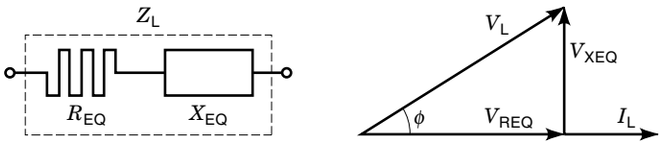

Figure 2. Voltage drop across the load and across its equivalent components.

this situation the active power is expressed as

$$P = V_1 I_1 \cos\phi_1 + V_5 I_5 \cos\phi_5$$

—that is, the actual power measurement is not affected by the 3rd, 5th, and 9th voltage harmonics or by the 11th current harmonic. In case of absence of distortion on either the voltage or the current, only the multiplication of the two fundamental waves must be performed.

The apparent power of nonsinusoidal waves is the product of the load voltage and current rms values:

$$P_A = V_L I_L = \sqrt{\sum_{h=0}^{M} V_h^2 \sum_{k=0}^{M} I_k^2} = \sqrt{V_0^2 I_0^2 + \sum_{h=1}^{M} V_h^2 I_h^2 + \sum_{\substack{h=1 \\ (h\neq k)}}^{M} \sum_{k=1}^{M} V_h^2 I_k^2} \tag{13}$$

where every voltage frequency component is separately combined with every current frequency component; the total apparent power then is not equal to the sum of the components related to the separate harmonics.

In the absence of the dc term, the difference $P_A^2 - P^2$ is

$$\begin{aligned}
P_A^2 - P^2 &= \sum_{h=1}^{M} V_h^2 I_h^2 + \sum_{\substack{h=1 \\ (h\neq k)}}^{M} \sum_{k=1}^{M} V_h^2 I_k^2 - \sum_{h=1}^{M} V_h^2 I_h^2 \cos^2 \Phi_h \\
&\quad - \sum_{\substack{h=1 \\ (h\neq k)}}^{M} \sum_{k=1}^{M} V_h I_h V_k I_k \cos\Phi_h \cos\Phi_k \\
&= \sum_{h=1}^{M} V_h^2 I_h^2 \sin^2 \Phi_h + \sum_{\substack{h=1 \\ (h\neq k)}}^{M} \sum_{k=1}^{M} V_h^2 I_k^2 \\
&\quad - \sum_{\substack{h=1 \\ (h\neq k)}}^{M} \sum_{k=1}^{M} V_h I_h V_k I_k \frac{\cos(\Phi_h - \Phi_k) + \cos(\Phi_h + \Phi_k)}{2} \\
&= \sum_{h=1}^{M} V_h^2 I_h^2 \sin^2 \Phi_h + \sum_{\substack{h=1 \\ (h\neq k)}}^{M} \sum_{k=1}^{M} V_h^2 I_k^2 \\
&\quad + \sum_{\substack{h=1 \\ (h\neq k)}}^{M} \sum_{k=1}^{M} V_h I_h V_k I_k \\
&\quad \frac{\cos(\Phi_h - \Phi_k) - \cos(\Phi_h + \Phi_k) - 2\cos(\Phi_h - \Phi_k)}{2} \\
&= \sum_{h=1}^{M} V_h^2 I_h^2 \sin^2 \Phi_h + \sum_{\substack{h=1 \\ (h\neq k)}}^{M} \sum_{k=1}^{M} V_h^2 I_k^2 \\
&\quad + \sum_{\substack{h=1 \\ (h\neq k)}}^{M} \sum_{k=1}^{M} V_h I_h V_k I_k [\sin\Phi_h \sin\Phi_k - \cos(\Phi_h - \Phi_k)] \\
&= \left(\sum_{h=1}^{M} V_h I_h \sin\Phi_h \right)^2 \\
&\quad + \sum_{\substack{h=1 \\ (h\neq k)}}^{M} \sum_{k=1}^{M} [V_h^2 I_k^2 - V_h I_h V_k I_k \cos(\Phi_h - \Phi_k)]
\end{aligned} \tag{14}$$

The first part of this relation contains terms involving the product of component of the same frequency; by analogy with the sinusoidal case, they can be expressed as

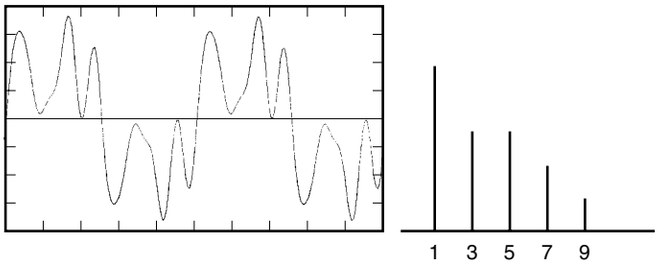

Figure 3. Voltage waveform in both time and frequency domains.

$$Q = \sum_{h=1}^{M} V_h I_h \sin\Phi_h \tag{15}$$

and called reactive power. This relation has no physical meaning, but it is a convenient analytical component introduced for its duality with the physical relation Eq. (8). This mathematical decomposition can be given various interpretations. Many other analytical decompositions are possible.

The second part of the relation contains the summation of the products of current and voltage harmonics with different frequencies, expressed in terms of a further analytical expression

$$D = \sqrt{P_A^2 - (P^2 + Q^2)} \tag{16}$$

and called the *distortion power*.

While in sinusoidal conditions the reactive power is entirely related to the energy storage, and in a system their components can be summed algebraically, this is not true in nonsinusoidal conditions. In the case of voltage components of order 1, 3, 5 and current components of order 1, 5, and 11,

$$\begin{aligned}
P_A^2 &= (V_1^2 + V_3^2 + V_5^2)(I_1^2 + I_5^2 + I_{11}^2) \\
P^2 &= V_1^2 I_1^2 \cos^2\phi_1 + V_5^2 I_5^2 \cos^2\phi_5 + 2V_1^2 I_1^2 V_5^2 I_5^2 \cos\phi_1 \cos\phi_5 \\
P_A^2 - P^2 &= V_1^2 I_1^2 + V_3^2 I_1^2 + V_5^2 I_1^2 + V_1^2 I_5^2 + V_3^2 I_5^2 + V_5^2 I_5^2 + V_1^2 I_{11}^2 \\
&\quad + V_3^2 I_{11}^2 + V_5^2 I_{11}^2 - V_1^2 I_1^2 \cos^2\phi_1 - V_5^2 I_5^2 \cos^2\phi_5 \\
&\quad - 2V_1^2 I_1^2 V_5^2 I_5^2 \cos\phi_1 \cos\phi_5 \\
&= V_1^2 I_1^2 \sin^2\phi_1 + V_5^2 I_5^2 \sin^2\phi_5 + V_3^2 I_1^2 + V_5^2 I_1^2 + V_1^2 I_5^2 \\
&\quad + V_3^2 I_5^2 + V_1^2 I_{11}^2 + V_3^2 I_{11}^2 + V_5^2 I_{11}^2 - 2V_1^2 I_1^2 V_5^2 I_5^2 \\
&\quad \cos\phi_1 \cos\phi_5
\end{aligned}$$

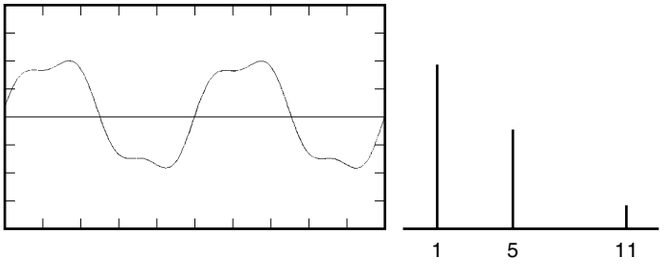

Figure 4. Current waveform in both time and frequency domains.

Voltage and current harmonics produce annoying effects in electrical power systems and also cause problems in industrial and communication apparatus. It is thus frequently necessary, or useful, to measure and analyze the power components in nonsinusoidal conditions.

High-Frequency Circuits. At low frequencies the power measurement is derived from voltage and current measurements. As the frequency increases, the wavelength become comparable to or lower than the circuit dimensions. In this case current and voltage become hard to measure, because they vary with the position along the transmission line, while the power remains constant. For this reason the power level is the most important factor in the design of high-frequency devices.

Power transmitted from a supply to a load at radio or microwave frequencies is generally measured by attaching a power sensor to the transmission-line port under measurement. The sensor output is connected to a power meter.

While an ideal sensor absorbs all the incident power (P_I), the actual impedance mismatch between the characteristic impedance of the radio frequency (RF) transmission line and the RF sensor input produces a partial reflection of the incoming power toward the supply. For this reason, the meter connected to the sensor does not account for the total amount of reflected power (P_R). The relationship among power dissipated in the load (P_L), power incident, and power reflected is obviously $P_L = P_I - P_R$.

Directional couplers allow separate measurement of incident and reflected power by means of power meters applied, respectively, on the right and on the left side of the secondary waveguide. Directional couplers are also used to determine the *reflection coefficient* ρ of the sensor, which takes into account mismatch losses and is defined by

$$P_R = \rho^2 P_I \tag{17}$$

In order to take into account also the absorptive losses due to dissipation in the conducting walls of the sensor, leakage into instrumentation, power radiated into space, and so on, beside the reflection coefficient, the *effective efficiency* η_C of the sensor should also be considered. Generally, the reflection coefficient and effective efficiency are included in the *calibration factor* K, defined as

$$K = \eta_C(1 - \rho^2) \times 100\% \tag{18}$$

For instance, a calibration factor of 90% means that the meter will read 10% below the incident power. Generally calibration factors are specified by sensor manufacturers at different values of frequency.

GENERAL METHODS AND INSTRUMENTATION

As far as methods and instruments for power measurements are concerned, the problems involved change as the frequency of the power supply increases. Therefore, in the following, power measurement is discussed by considering general methods and instrumentation for dc and ac circuits. The ac circuits will be classified as (1) line-frequency circuits, (2) low- and medium-frequency circuits (up to a few megahertz), and (3) high-frequency circuits (up to a few gigahertz). Line-frequency circuits will be discussed separately from low-frequency circuits principally because of the existence of problems related specifically to three-phase power of the main.

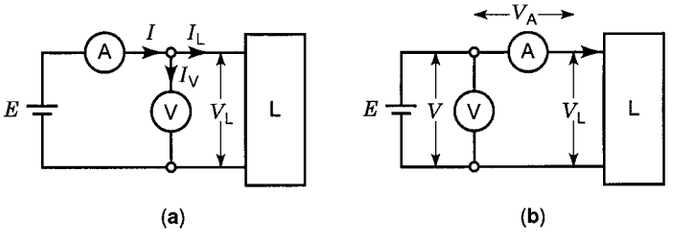

Figure 5. Two arrangements for dc power measurement circuits.

Dc Circuits

A power measurement in a dc circuit can be generally carried out by using a voltmeter (V) and an ammeter (A), according to one of the connections shown in Fig. 5.

Both the connections introduce a systematic error, generally referred to as insertion error. In the connection of Fig. 5(a) the ammeter measures the current flowing into the voltmeter, I_V, as well as that flowing into the load, I_L. In the connection of Fig. 5(b) the voltmeter measures the voltage drop across the load, V_L, in addition to that dropping across the ammeter, V_A. So both connections give an excess of measured power, representing the power absorbed by the instrument connected closer to the load.

The analysis of the circuits of Fig. 5(a,b) provides the relations between the measurand, the electrical power P in the load, and the measured voltage V and current I, expressed as

$$P = V_L I_L = V(I - I_V), \qquad P = V_L I_L = I(V - V_A) \tag{19}$$

By neglecting R_L (compared with the voltmeter internal resistance R_V) for the connection of Fig. 5(a) and the ammeter resistance R_A (compared with R_L) for the connection of Fig. 5(b), we have the respective approximations

$$I_V = I\frac{R_L}{R_V + R_L} \approx I\frac{R_L}{R_V}, \qquad V_A = V\frac{R_A}{R_A + R_L} \approx V\frac{R_A}{R_L} \tag{20}$$

Consequently, the equations (19) become respectively

$$\begin{aligned} P &= VI\left(1 - \frac{R_L}{R_V}\right) = VI\frac{R_V - R_L}{R_V} \\ P &= VI\left(1 - \frac{R_A}{R_L}\right) = VI\frac{R_L - R_A}{R_L} \end{aligned} \tag{21}$$

From Eqs. (20) and (21) analytical corrections of the insertion errors can be easily derived.

In a dc circuit the electrical power can also be measured by a wattmeter. The instrument most commonly used is the dynamometer. It is made of two fixed coils, positioned coaxially with space between them, and a moving coil, placed be-

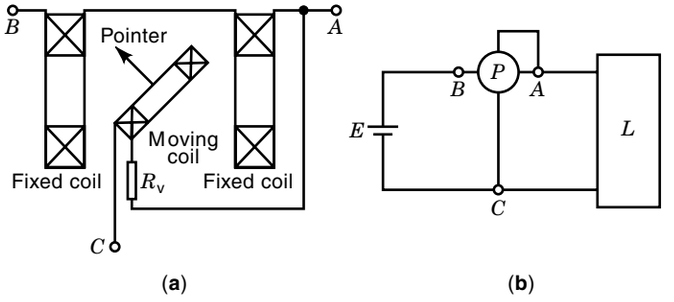

Figure 6. Power measurement with a dynamometer: (a) working principle, (b) measurement circuit.

tween the fixed coils and equipped with a pointer [Fig. 6(a)]. The fixed coils, commonly known as *current coils,* are connected in series with the load, to carry the load current. The moving coil (*voltage coil*), with a resistor R_V in series, is connected in parallel with the load R_L, to carry a current proportional to the voltage across it. When each coil carries a current, the interaction between the magnetic fields produced by the fixed and moving coils supplies a torque to move the pointer, which is proportional to the product of the two currents flowing into the coils. As a consequence, the deflection of the moving coil is proportional to the power dissipated in the load.

Insertion errors are also present in the dynamometer power measurement. In particular, on connecting the voltage coil between A and C [Fig. 6(b)], the current coils carry both the current through the load and that taken by the voltage coil. Consequently, the power P_L dissipated in the load can be obtained from the dynamometer reading P as

$$P_L = P - \frac{V^2}{R'_V} \tag{22}$$

where $R'_V = R_V + R_{VC}$ is the overall resistance of the voltage circuit (R_{VC} is the resistance of the voltage coil). By connecting the moving coil between B and C, this current error can be avoided, but now the voltage coil measures the excess voltage drop across the current coils. In this case the power in the load is

$$P_L = P - I^2 R_C \tag{23}$$

where R_C is the resistance of the current coil.

Ac Circuits

Active power in ac circuits can be measured by a dynamometer. Since its moving system cannot follow the rapid torque variations, it works as an intrinsic integrator of the instantaneous power, showing the average power according to Eq. (5). The insertion errors can be derived by simple considerations, in analogy with the previously discussed dc case, by replacing voltages and currents by the corresponding rms values.

However, a phase uncertainty due to the self-inductance of the voltage circuit arises in ac measurements. In sinusoidal conditions, if e_ω (in radians) is the phase defect angle (departure from exact quadrature) of the voltage circuit and cos ϕ the load power factor, the relative uncertainty in active power measurements can be shown to be equal to $-e_\omega \tan \phi$. The phase uncertainty depends on the frequency. By using more complex circuits to compensate for this source of error, the frequency range of the dynamometer can be extended up to a few tens of kilohertz.

The reactive power measurement can be carried out by using special instruments (varmeters or reactive meters) with the same arrangements described for the active power. These are instruments whose response is proportional to $V_L I_L \sin \phi = V_L I_L \cos (90° - \phi)$, where cos ϕ is the load power factor. It can be measured with a wattmeter, by shifting the line voltage into quadrature.

In a polyphase system reactive power can be derived from the readings of wattmeters connected in a special way (Barbagelata's and Righi's insertions; see "Symmetrical Power Systems Supplying Unbalanced Loads" below). Also the apparent power, which is important for determining the line and supply capacity, can be measured by using a voltmeter and an ammeter. Electronic instruments, such as sampling wattmeters, can generally process the acquired data to supply all the different power quantities.

Line Frequency

For applications where the power is directly derived from the mains, the assumption of infinite power source can be reliably made and at least one of the two quantities voltage and current can be considered as sinusoidal. In this case only the power at the fundamental frequency should be examined (1).

Single-Phase Measurement. The power measurement at line frequency in single-phase circuits is generally carried out by a dynamometer, though the use of electronic instruments has become common. In practical applications, the case of a voltage greater than 1000 V is very common. Then the measurement must be carried out by using voltage and current transformers, inserted as shown in Fig. 7. In this case, the relative measurement uncertainty is equal to

$$\frac{\Delta P}{P} = (\eta_w + \eta_a + \eta_v) + (\epsilon_w + \epsilon_a + \epsilon_v) \tan \Phi_c \tag{24}$$

where η_w and ϵ_w are the instrumental and phase uncertainty of the wattmeter, η_a and η_v are the ratio uncertainties of the

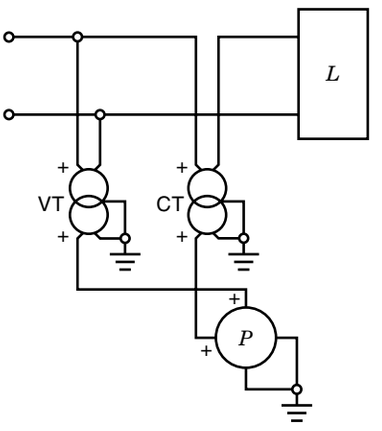

Figure 7. Single-phase power measurement with voltage (VT) and current (CT) transformers.

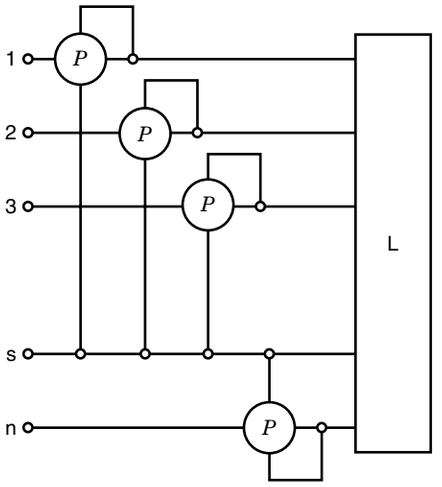

Figure 8. Power measurement on systems with several wires.

current (CT) and voltage (VT) transformers, and ϵ_a and ϵ_v are their phase uncertainties, respectively. If the load current exceeds the current range of the wattmeter, a current transformer has to be used, even in the case of low voltages.

Polyphase Power Measurement. In the following, the general case of power measurements on polyphase systems is analyzed. The common case of three-phase systems is treated, and different solutions are considered.

Measurements on Systems with Several Wires. Let a network with sinusoidal voltages and currents composed of n wires be considered. Among the currents flowing in such wires the following relation is established:

$$\sum_{i=1}^{n} \dot{I} = 0 \tag{25}$$

The network can be thought as composed of n-1 single-phase independent systems, with the common return on one of the wires (say the sth wire). Then the total power can be measured as the sum of the readings of n-1 wattmeters, each one inserted with the current circuit in a different wire and the voltmeter circuit between that wire and the sth one (Fig. 8):

$$P = \sum_{i \neq s}^{n} \dot{V}_{is} \dot{I}_i \tag{26}$$

The load power can also be measured by referring to a generic point O external to the network, as the sum of the readings of n wattmeters, each inserted with the ammeter circuit in a different wire and the voltmeter circuit connected between that wire and the point O:

$$P = \sum_{i=1}^{n} \dot{V}_{iO} \dot{I}_i \tag{27}$$

Power Measurements on Three-Wire Systems. The active power in a three-phase power system can generally be evaluated with three wattmeters connected as shown in Fig. 9. On each instrument, the current system is connected to carry the line current, while the voltmeter system is connected between the same wire and an artificial neutral point O, whose position is fixed by the voltmeter impedance of wattmeters or by suitable external impedances.

In these conditions the power in the load is the sum of the three wattmeters' indications:

$$P = \sum_{i=1}^{3} \dot{V}_{iO} \dot{I}_i \tag{28}$$

If the three-phase system is provided by four wires (three phases with a neutral wire), the neutral wire is utilized as the common wire.

Analogously to the single-phase case, for medium-voltage circuits the three-wattmeter insertion is modified as in Fig. 10.

Symmetrical and Balanced Systems. The supply system is symmetrical and the three-phase load is balanced if

$$\begin{aligned} V_1 &= V_2 = V_3 \\ I_1 &= I_2 = I_3 \end{aligned} \tag{29}$$

In Fig. 11 the three possible kinds of insertion of an instrument S (active or reactive power meter) are illustrated, by using the following convention: S_{ijk} indicates a reading performed with the current leads connected to line i and the voltmeter leads connected between phases j and k. If i is equal to j, one is omitted, for example, P_{12} [Fig. 11(b)]. The active power related to a single phase is usually referred to as P_1.

In the first case [Fig. 11(a)] S is inserted between the phase and the artificial point O. By Eq. (29), the overall active power is given by three times the indication of the wattmeter S; similarly for the overall reactive power if S is a reactive power meter. Notice that a pair of twin resistors with the same resistance R as that of the voltage circuit of S are placed on the other phases in order to balance the load.

The wattmeter reading corresponding to Fig. 11(c) can be expressed as

$$P_{1(23)} = \dot{I}_1 \dot{V}_{23} \tag{30}$$

But $\dot{V}_{12} + \dot{V}_{23} + \dot{V}_{31} = 0$ and $\dot{V}_{13} = -\dot{V}_{31}$; thus

$$P_{1(23)} = \dot{I}_1(-\dot{V}_{12} - \dot{V}_{31}) = -\dot{I}_1 \dot{V}_{12} + \dot{I}_1 \dot{V}_{13}$$

where the last two terms are $\dot{I}_1 \dot{V}_{12} = P_{12}$ and $\dot{I}_1 \dot{V}_{13} = P_{13}$, which

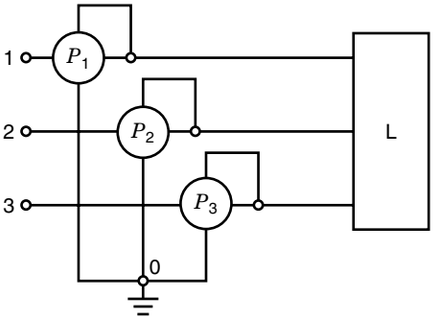

Figure 9. Insertion of three wattmeters for three-wire three-phase systems.

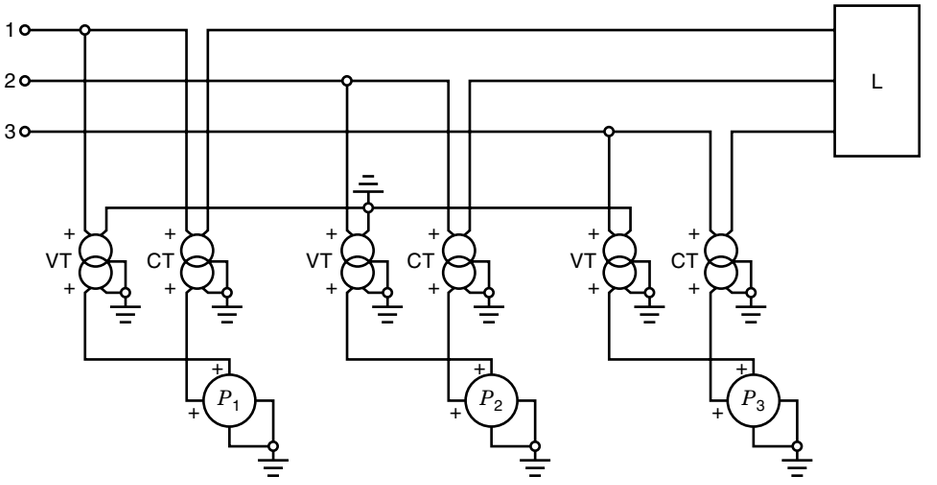

Figure 10. Insertion of three wattmeters for medium voltage.

lead to the final relation, and to corresponding relations for the other phases, valid for any kind of supply and load:

$$\begin{aligned} P_{1(23)} &= P_{13} - P_{12} \\ P_{2(31)} &= P_{21} - P_{23} \\ P_{3(12)} &= P_{32} - P_{31} \end{aligned} \tag{31}$$

If the supply system is symmetrical, we have $P_{1(23)} = \sqrt{3}\, Q_1$. In fact, starting from the relationship

$$P_{1(23)} = \dot{I}_1 \dot{V}_{23} = I_1 V_{23} \cos\beta \tag{32}$$

where $\beta = 90° - \phi_1$ (Fig. 12), we have

$$P_{1(23)} = \sqrt{3} E_1 I_1 \sin\phi_1 = \sqrt{3} Q_1$$

with Q_1 the reactive power involved in phase 1. The three final relationships are

$$\begin{aligned} P_{1(23)} &= \sqrt{3} Q_1 = P_{13} - P_{12} \\ P_{2(31)} &= \sqrt{3} Q_2 = P_{21} - P_{23} \\ P_{3(12)} &= \sqrt{3} Q_3 = P_{32} - P_{31} \end{aligned} \tag{33}$$

Hence, in the case of symmetrical and balanced systems, the overall reactive power is given by

$$Q = 3Q_1 = 3P_{1(23)}/\sqrt{3} = \sqrt{3} P_{1(23)} \tag{34}$$

Power Measurements Using Two Wattmeters. The overall active power in a three-wire system can be measured by using only two wattmeters. In fact, Aron's theorem states the following relationships:

$$\begin{aligned} P &= P_{12} + P_{32} \\ P &= P_{23} + P_{13} \\ P &= P_{31} + P_{21} \end{aligned} \tag{35}$$

Analogously, the overall reactive power can be measured by using only two reactive power meters:

$$\begin{aligned} Q &= Q_{12} + Q_{32} \\ Q &= Q_{23} + Q_{13} \\ Q &= Q_{31} + Q_{21} \end{aligned} \tag{36}$$

To prove one of the previous statements, say $P = P_{12} + P_{32}$, refer to Fig. 13, where the two wattmeters furnish P_{12} and

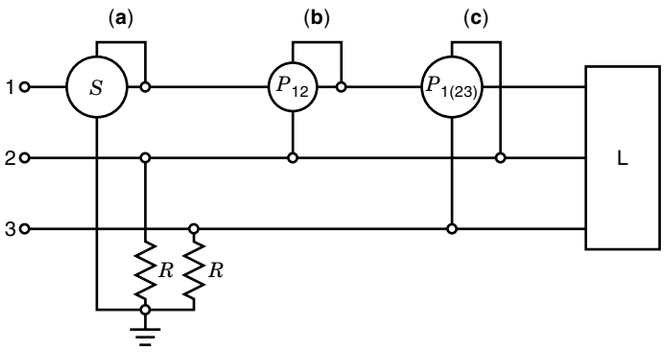

Figure 11. The three modes of insertion of a power meter.

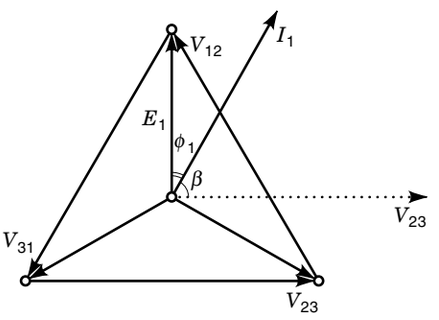

Figure 12. Phasor diagram for a three-phase symmetrical and balanced system.

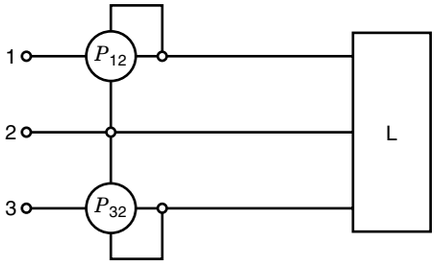

Figure 13. Power measurements using two wattmeters.

P_{32}. Hence the sum of the two readings gives

$$\begin{aligned} P_{12}+P_{32} &= \dot{I}_1\dot{V}_{12}+\dot{I}_3\dot{V}_{32} = \dot{I}_1(\dot{E}_1-\dot{E}_2)+\dot{I}_3(\dot{E}_3-\dot{E}_2) \\ &= \dot{I}_1\dot{E}_1-\dot{I}_1\dot{E}_2+\dot{I}_3\dot{E}_3-\dot{I}_3\dot{E}_2 \\ &= \dot{I}_1\dot{E}_1+\dot{I}_3\dot{E}_3-(\dot{I}_1+\dot{I}_3)\dot{E}_2 \\ &= \dot{I}_1\dot{E}_1+\dot{I}_3\dot{E}_3+\dot{I}_2\dot{E}_2 = P_1+P_2+P_3 = P \end{aligned} \tag{37}$$

Provided that the system has only three wires, Aron's theorem applies to any kind of supply and load. In the case of symmetrical and balanced systems, it also allows the reactive power to be evaluated as

$$Q = \sqrt{3}(P_{32}-P_{12}) \tag{38}$$

By using Eqs. (35) and (38) the power factor is seen to be

$$\begin{aligned} \cos\phi &= \frac{P_{12}+P_{32}}{\sqrt{(P_{12}+P_{32})^2+3(P_{32}-P_{12})^2}} \\ &= \frac{P_{12}+P_{32}}{\sqrt{4P_{12}^2+4P_{32}^2-4P_{12}P_{32}}} \\ &= \frac{1+(P_{12}/P_{32})}{2\sqrt{(P_{12}/P_{32})^2-(P_{12}/P_{32})+1}} \end{aligned} \tag{39}$$

Aron's insertion presents a limitation for low power factors. In fact, considering the functions

$$\begin{aligned} \cos(\phi+30^\circ) &= \frac{P_{12}}{VI} \\ \cos(\phi-30^\circ) &= \frac{P_{32}}{VI} \end{aligned} \tag{40}$$

(Fig. 14), it can be argued that for $\phi \le 60^\circ$, P_{12} and P_{32} are both greater than zero, while for $\phi > 60^\circ$, $\cos(\phi - 30^\circ)$ is still

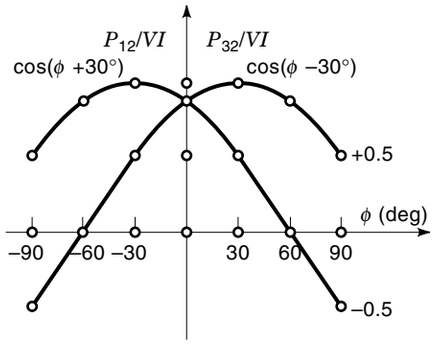

Figure 14. Sign of powers in Aron's insertion.

greater than zero and $\cos(\phi + 30^\circ)$ is less than zero. The absolute error in the active power is

$$\Delta P = \frac{\partial(P_{12}+P_{32})}{\partial P_{12}}\Delta P_{12} + \frac{\partial(P_{12}+P_{32})}{\partial P_{32}}\Delta P_{32} = \Delta P_{12}+\Delta P_{32} \tag{41}$$

This corresponding relative error is greatest when P_{12} and P_{32} have values close to each other and opposite in sign; in particular, for $\cos\phi = 0$ ($\phi = 90^\circ$) the error is infinite.

If η_w and ϵ_w are the wattmeter amplitude and phase errors, the error in the active power is

$$\frac{\Delta P}{P} = \frac{(\eta_w+\epsilon_w\tan\phi_{12})P_{12}+(\eta_w+\epsilon_w\tan\phi_{32})P_{32}}{P_{12}+P_{32}} = \eta_w+\epsilon_w\frac{Q}{P} \tag{42}$$

Let two wattmeters with nominal values V_0, I_0, $\cos\phi_0$ and accuracy class c be considered. The maximum absolute error in each reading is

$$\Delta P = \frac{cV_0I_0\cos\phi_0}{100} \tag{43}$$

Therefore, the percentage error related to the sum of the two indications is

$$\frac{\Delta P}{P} = \frac{cV_0I_0\cos\phi_0}{\sqrt{3}VI\cos\phi} = 1.11\frac{cV_0I_0\cos\phi_0}{VI\cos\phi} \tag{44}$$

equal approximately to the error of only one wattmeter inserted in a single-phase circuit with the same values of I, V, and $\cos\phi$. Consequently, under the same conditions, the use of two wattmeters involves a measurement uncertainty rather lower than the use of three wattmeters. If the Aron's insertion is performed via current and voltage transformers, characterized by ratio errors η_a and η_v and phase errors ϵ_a and ϵ_v respectively, the active power error is

$$\begin{aligned} \frac{\Delta P}{P} &= \frac{(\eta_{TOT}+\epsilon_{TOT}\tan\phi_{12})P_{12}+(\eta_{TOT}+\epsilon_{TOT}\tan\phi_{32})P_{32}}{P_{12}+P_{32}} \\ &= \eta_{TOT}+\epsilon_{TOT}\frac{Q}{P} = \eta_{TOT}+\epsilon_{TOT}\tan\Phi_c \end{aligned} \tag{45}$$

where $\cos\phi_c$ is the conventional power factor, and

$$\begin{aligned} \eta_{TOT} &= \eta_w+\eta_a+\eta_v \\ \epsilon_{TOT} &= \epsilon_w+\epsilon_a+\epsilon_v \end{aligned}$$

the error sums, with η_w, ϵ_w the wattmeter errors.

Symmetrical Power Systems Supplying Unbalanced Loads. If the load is unbalanced, the current amplitudes are different from each other and their relative phase is not equal to 120°. In this situation two wattmeters and one voltmeter have to

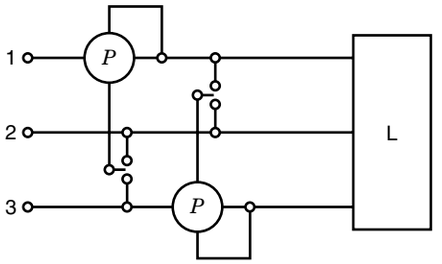

Figure 15. Barbagelata's insertion for symmetrical and unbalanced systems.

be connected as proposed by Barbagelata (1) (Fig. 15). The first wattmeter gives P_{12} and P_{13} (changing the switch position), and the second one gives P_{31} and P_{32}.

From Aron's theorem the active power is

$$P = P_{12} + P_{32} \tag{46}$$

and then the reactive power Q is

$$Q = Q_1 + Q_2 + Q_3 = \frac{1}{\sqrt{3}}(P_{13} - P_{12} + \underline{P_{21}} - \underline{P_{23}} + P_{32} - P_{31}) \tag{47}$$

For the underlined terms, from Aron's theorem it follows that

$$P = P_{13} + P_{23} = P_{12} + P_{32} = P_{21} + P_{31} \tag{48}$$

Then

$$P_{13} + P_{23} = P_{21} + P_{31} \qquad \text{so} \quad P_{21} - P_{23} = P_{13} - P_{31}$$

Then we have

$$Q = \frac{1}{\sqrt{3}}[2(P_{13} - P_{31}) + P_{32} - P_{12}] \tag{49}$$

Hence, from only four power measurements, the overall active and reactive powers can be obtained.

The main disadvantage of this method is that the four measurements are not simultaneous; therefore, any load variations during the measurement will cause a loss in accuracy. In this case, a variation proposed by Righi (1) may be used, with three wattmeters connected as shown in Fig. 16 to measure P_{12}, P_{32}, and $P_{2(31)}$ simultaneously. The reactive power is

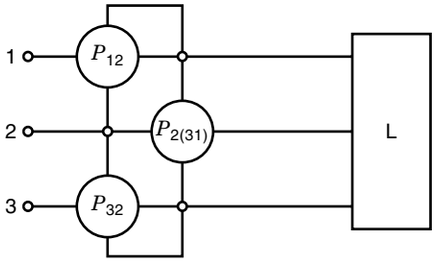

Figure 16. Righi's insertion for symmetrical and unbalanced systems.

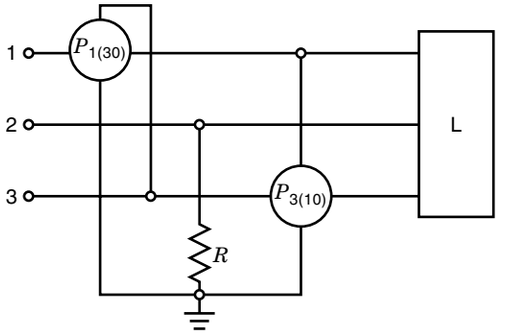

Figure 17. Insertion of two wattmeters for symmetrical and unbalanced systems.

$$Q = \frac{1}{\sqrt{3}}(\underline{P_{13}} - P_{12} + P_{21} - P_{23} + P_{32} - \underline{P_{31}}) \tag{50}$$

As above, from Aron's theorem it follows that

$$P_{21} - P_{23} = P_{13} - P_{31} \quad \text{and} \quad P_{2(31)} = P_{21} - P_{23} = P_{13} - P_{31}$$

Then

$$Q = \frac{1}{\sqrt{3}}(P_{32} - P_{12} + 2P_{2(31)}) \tag{51}$$

For symmetrical and unbalanced systems another two-wattmeter insertion can be carried out (Fig. 17). The wattmeters give

$$\begin{aligned} P_{1(30)} &= \dot{E}_3\dot{I}_1 = j\frac{\dot{V}_{12}}{\sqrt{3}}\dot{I}_1 = -\frac{Q_{12}}{\sqrt{3}} \\ P_{3(10)} &= \dot{E}_1\dot{I}_3 = j\frac{\dot{V}_{23}}{\sqrt{3}}\dot{I}_3 = \frac{Q_{32}}{\sqrt{3}} \end{aligned} \tag{52}$$

Hence, the overall reactive power is

$$Q = Q_{12} + Q_{32} = \sqrt{3}(-P_{1(30)} + P_{3(10)}) \tag{53}$$

Method Selection Guide. For three-wire systems, the flux diagram of Fig. 18 leads to selecting the most suitable method according to system characteristics.

Low- and Medium-Frequency Power Measurements

In the following, the main methods and instruments for power measurements at low and medium frequencies are considered.

Three-Voltmeter Method. The power dissipation in the load L can be measured by using a non-inductive resistor R and three voltmeters, as shown in Fig. 19 (2). Though one of the voltmeters may appear redundant on a first analysis of the circuit, in actual fact three independent data are needed in order to derive the power from Eq. (7). In particular, from the voltage drops v_{AB} and v_{BC}, the load current and load voltage can be directly derived; then, v_{AC} is used to retrieve informa-

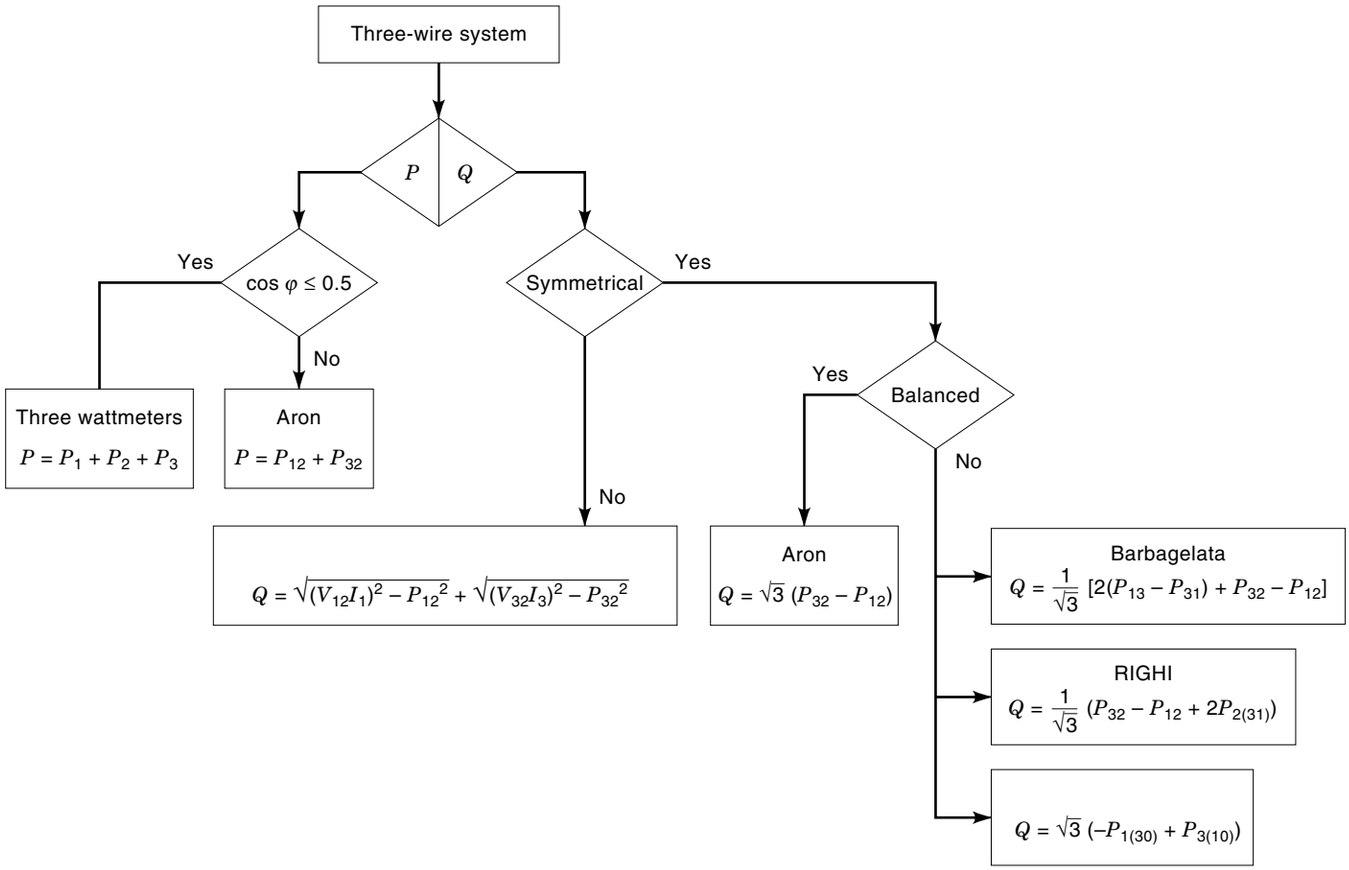

Figure 18. Method selection guide for power measurements on three-wire systems.

tion about their relative phase. If the currents drawn by the voltmeters are neglected and the current i_L flowing into the load L is assumed to be equal to that flowing into the resistor R, the statement can be demonstrated as follows:

$$\begin{aligned} v_{AC} &= Ri_L + v_L \\ v_{AC}^2 &= R^2 i_L^2 + v_L^2 + 2Rv_L i_L \end{aligned} \tag{54}$$

where the lowercase letters indicate instantaneous values. By computing rms values (indicated with capital letters) we obtain the power P_L:

$$\frac{1}{T}\int_0^T v_{AC}^2\,dt = \frac{1}{T_0}\int_0^T R^2 i_L^2\,dt + \frac{1}{T}\int_0^T v_L^2\,dt + \frac{1}{T}\int_0^T 2Rv_L i_L\,dt$$

$$V_{AC}^2 = R^2 I_L^2 + V_L^2 + 2RP_L$$

$$P_L = \frac{V_{AC}^2 - R^2 I_L^2 - V_L^2}{2R} = \frac{V_{AC}^2 - V_{AB}^2 - V_{BC}^2}{2R} \tag{55}$$

The expression (55) is also applicable to dc on replacing rms values with dc ones. Since the result is obtained as a difference, problems arise from relative uncertainty when the three terms have a sum near zero.

Such a method is still used for high-accuracy applications.

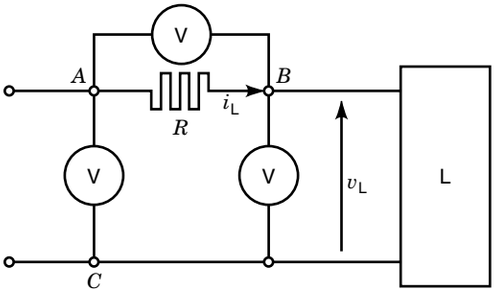

Figure 19. Three-voltmeter method.

Thermal Wattmeters. The working principle of thermal wattmeters is based on a pair of twin thermocouples whose output voltage is proportional to the square of the rms value of the currents flowing into the thermocouple heaters (3).

The essential circuit of a thermal wattmeter is shown in Fig. 20(a). Without the load, if the two heaters have equal resistance ($r_1 = r_2 = r$), in the limit $S \ll r$ they are connected in parallel and carry the same current i_p, proportional to the supply voltage:

$$i_1 = i_2 = i_p = \frac{v}{2R + r} \tag{56}$$

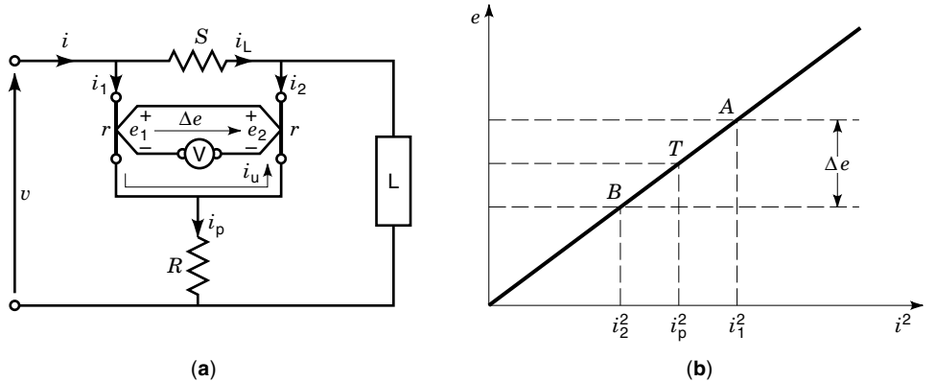

Figure 20. (a) Thermal wattmeter based on twin thermocouples; (b) working characteristic in ideal conditions.

In this case, the output voltages of the two thermocouples turn out to be equal ($e_1 = e_2$), thus the voltage Δe measured by the voltmeter is null. In Fig. 20(b) this situation is represented by the working point T, the same for both thermocouples. By applying a load L with a corresponding current i_L, a voltage drop across S arises, determining an imbalance between currents i_1 and i_2 (i_1 increases and i_2 decreases). In the limit $r \ll R$, the two heaters are in series; thus the current imbalance i_u through them is proportional to the load current:

$$i_u = i_1 - i_2 = \frac{S}{2R} i_L \tag{57}$$

Therefore, the working points of the two thermocouples change: to A for the thermocouple that carries the current i_1, and to B for the other one [Fig. 20(b)].

Because the thermocouple response time is higher than the period of the heater current, it produces an emf proportional to the average squared value of this current. In this situation, in the above *limits,* the voltmeter measures a voltage imbalance Δe proportional to the active power absorbed by the load (except for the excess given by the powers dissipated in R, S, r_1, and r_2):

$$\Delta e = k(\overline{i_1^2} - \overline{i_2^2}) = k[\overline{(i_p + i_L)^2} - \overline{(i_p - i_L)^2}] = k$$
$$\overline{4 i_p i_L} = k_1 \overline{v(t) i(t)} = k_1 P \tag{58}$$

where the overbars indicate time averages.

If the two thermocouples cannot be considered as matched and linear, the power measurement accuracy will obviously be compromised. This situation is shown in Fig. 21, where the two thermocouples are supposed to have two quite different nonlinear characteristics. In this case, the voltage measured by the voltmeter will be Δe_n instead of Δe.

Wattmeters based on the thermal principle allow high accuracy to be achieved in critical cases of highly distorted wideband signals.

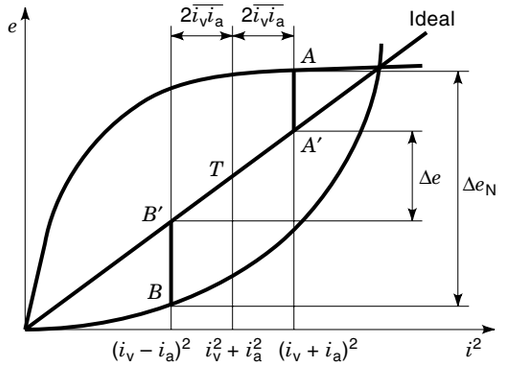

Figure 21. Ideal and actual characteristics of thermal-wattmeter thermocouples.

Wattmeters Based on Multipliers. The multiplication and averaging processes involved in power measurements can be undertaken by electronic circuits (Fig. 22). Wattmeters of this kind fall into two categories, depending on whether the multiplication and averaging operations are performed in a continuous or a discrete way. In the first case multiplication is usually carried out by means of an analog electronic multiplier, while averaging is carried out by a low-pass filter or by an averaging reading instrument. In the other case (sampling wattmeters), simultaneous samples of voltage and current waveforms are taken, digitized, and then multiplied and averaged by using digital techniques.

In multiplier methods also, the resistances of the voltage and current circuits have to be taken into account, analogously to the case of dynamometers [see Eqs. (22) and (23)]. Furthermore, phase errors of both current circuits ($e_{\omega c}$) and voltage circuits ($e_{\omega v}$) increase the relative uncertainty of power measurement [in the case of sinusoidal conditions by ($e_{\omega c} - e_{\omega v}$) tan ϕ].

Wattmeters Based on Analog Multipliers. The main analog multipliers are based on a transistor circuit, such as a four-quadrant multiplier (4), which is fed by voltage and current signals to give the instantaneous power, and an integrator to provide the mean power (Fig. 23). More effective solutions are based on the time-division multiplier (TDM) and on Hall-effect-based multipliers.

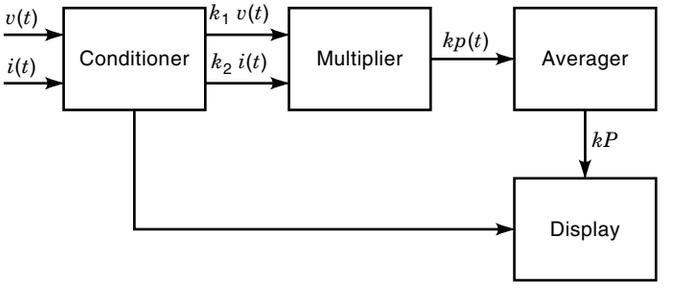

Figure 22. Block diagram of a multiplier-based wattmeter.

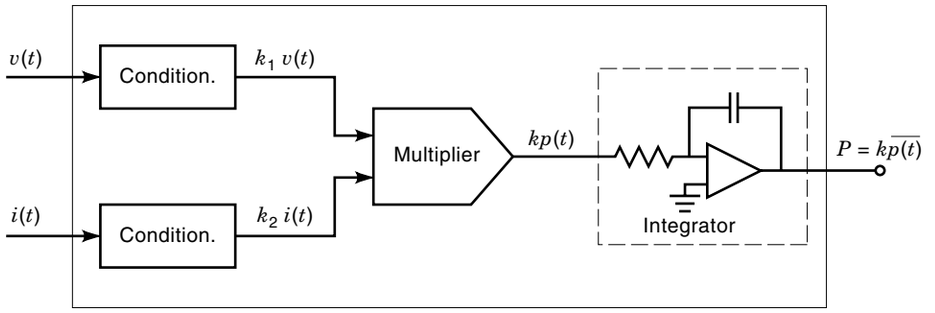

Figure 23. Block diagram of a four-quadrant multiplier-based wattmeter.

TDM-Based Wattmeters. The block diagram of a wattmeter based on a TDM is shown in Fig. 24 (5). A square wave v_m [Fig. 25(a)] with constant period T_g, and with duty cycle and amplitude determined by $i(t)$ and $v(t)$, respectively, is generated. T_g is much smaller than the period of the measurands $v_x(t)$ and $v_i(t)$, so that one can consider these voltages constant during that time interval.

The duty cycle of v_m is set by the impulse duration modulator circuit (Fig. 24). The ramp voltage $v_g(t)$ [Fig. 25(b)], compared with the voltage $v_i(t)$ proportional to $i(t)$, produces a square-wave output, which drives the switch SW, fixing a time interval t_2 of the output $v_m(t)$ proportional to $v_i(t)$. If

$$v_g(t) = \frac{4V_{g0}}{T_g}t \qquad \text{when} \quad 0 \le t \le \frac{T_g}{4} \tag{59}$$

from simple geometrical considerations we obtain

$$t_2 = 2\left(\frac{T_g}{4} - \frac{T_g}{4}\frac{v_i}{V_{g0}}\right) \tag{60}$$

and

$$t_1 - t_2 = \frac{T_g}{V_{g0}}v_i \tag{61}$$

The amplitude of $v_m(t)$ is set by the impulse amplitude modulator circuit to be equal to $+v_x$ during the time interval t_1, and to $-v_x$ during the time interval t_2 [Fig. 25(a)].

After an initial transient, the output voltage $v_{out}(t)$ of the low-pass filter (integrator) is the mean value of $v_m(t)$:

$$\begin{aligned} V_{out} &= \frac{1}{RC}\int_0^t v_m(t)\,dt = K'\left(\int_0^{t_1} v_x(t)\,dt - \int_{t_1}^{t_1+t_2} v_x(t)\,dt\right) \\ &= K'v_x(t_1 - t_2) = Kv_xv_i \end{aligned} \tag{62}$$

The frequency range is generally between 200 Hz and 20 kHz, but can reach 100 kHz. Uncertainties are typically 0.01% to 0.02% (6).

Hall-Effect Based Wattmeters. As is known, in a Hall-effect transducer the output voltage $v_H(t)$ is proportional to the product of two time-dependent quantities, the current $i(t)$ through the transducer and the magnetic induction $B(t)$ (7):

$$v_H(t) = R_H i(t)B(t) \tag{63}$$

where R_H is the Hall constant. In the circuit of Fig. 26(a), the power P is determined by measuring $v_H(t)$ through a high-input-impedance averaging voltmeter, and by considering that $v_x(t) = ai(t)$ and $i_x(t) = bB(t)$, with a and b proportionality

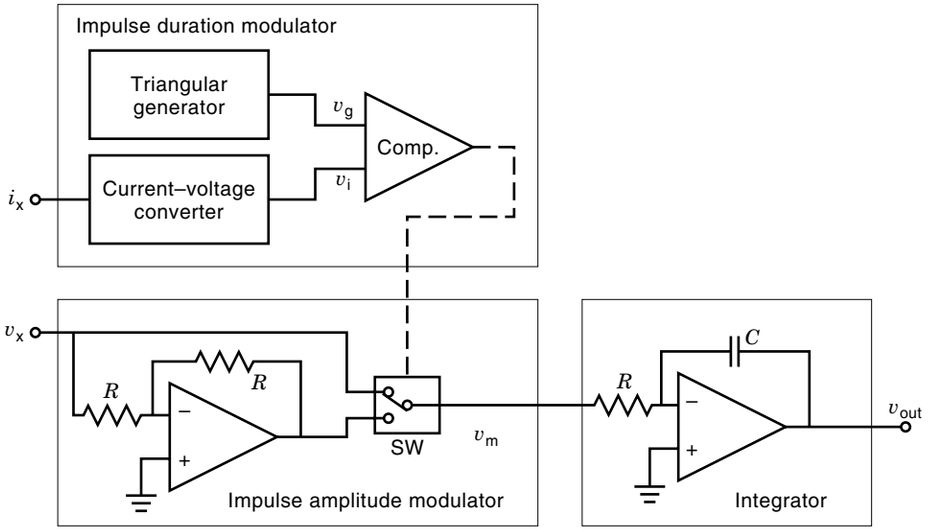

Figure 24. Block diagram of a TDM-based wattmeter.

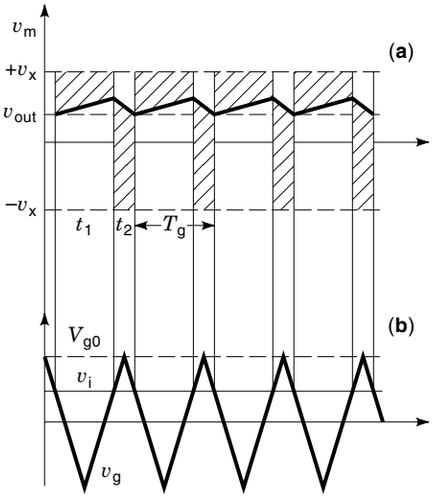

Figure 25. Waveform of TDM-based power measurement: (a) impulse amplitude-modulator output, (b) ramp-generator output.

factors:

$$P = \frac{1}{T}\int_0^T v_x(t) i_x(t)\,dt = ab\frac{1}{T}\int_0^T i(t)B(t)\,dt = ab\,\frac{V_H}{R_H} \quad (64)$$

where T is the measurand period, and V_H the mean value of $v_H(t)$.

In the usual realization of the Hall multiplier (accuracy 0.1% up to a few megahertz), shown in Fig. 26(a), the magnetic induction is proportional to the load current i_L and the optimal polarizing current i_v is set by the resistor R_v. For frequencies over the megahertz range, an alternative arrangement is shown in Fig. 26(b), in which the load current i_L, or a suitable amount of it reduced by inserting the shunt R_s, flows directly into the Hall device, acting as a polarizing current, and the magnetic field is generated by the voltage v_x. In this way, the influence of temperature is reduced for line-frequency applications with constant-amplitude voltages and variable load currents.

Standard wattmeters for high frequency, use probes in waveguides with rectifiers.

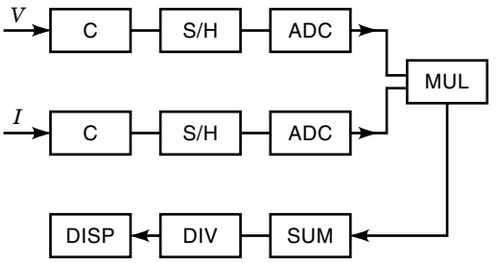

Figure 27. Block diagram of the sampling wattmeter.

Wattmeters Based on Digital Multipliers

Sampling Wattmeters. The most important wattmeter operating on discrete samples is the sampling wattmeter (Fig. 27). It is essentially composed of two input channels, each constituted by a conditioner (C), a sample–hold (S/H), and an analog-to-digital converter (ADC). Digital multiplier (MUL), summing (SUM), dividing (DIV), and displaying (DISP) units are also included. The architecture is handled by a processing unit, not shown in the figure.

The uniform sampling of input signals allows the active power to be evaluated as the mean of the sequence of instantaneous power samples $p_j(k)$:

$$P = \frac{1}{N}\sum_{k=0}^{N-1} p_j(k) = \frac{1}{N}\sum_{k=0}^{N-1} v_j(k) i_j(k) \quad (65)$$

where N is the number of samples in one period of the input signal. A previous estimation of the measurand fundamental period is made to adjust the summation interval of Eq. (65) and/or the sampling period in order to carry out synchronous sampling (8). The sampling period can be adjusted by using a frequency multiplier with a PLL circuit driven by the input signal (9). Alternatively, the contribution of the sampling error is reduced by averaging over a large number of periods of the input signal.

In the time domain, estimation of the period of highly distorted signals, as in pulse width modulation (PWM), is made difficult by the numerous zero crossings present in the waveform. Some types of digital filters can be used for this purpose. An efficient digital way to estimate the period is the

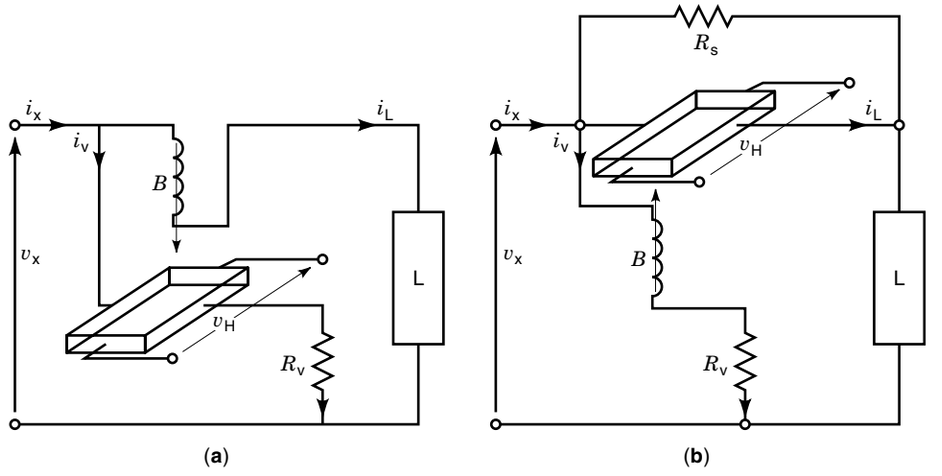

Figure 26. Configurations of the Hall-based wattmeter.

discrete integration of the PWM signal. In this way, the period of the fundamental harmonic is estimated by detecting the sign changes of the cumulative sum function (10):

$$S(k) = \sum_{i=1}^{k} v_i, \qquad k = 1, 2, \ldots, N \tag{66}$$

If the summation interval is extended to an integer number of periods of the function $S(k)$, then *quasisynchronous* sampling (11) is achieved through a few simple operations (cumulative summation and sign detection), and the maximum synchronization error is limited to a sampling period. Through relatively small increases in computational complexity and in memory size, the residual error can be further reduced through a suitable data-processing algorithm, that is, the multiple convolution in the time domain of triangular windows (10). Hence, the power measurement can be obtained as

$$P_{(B)} = \frac{1}{\sum_{k=0}^{2B(N-1)} w(k)} \sum_{k=0}^{2B(N-1)} w(k)p(k) \tag{67}$$

where $p(k)$ is the kth sample of the instantaneous power and $w(k)$ the kth weight corresponding to the window obtained as the convolution of B triangular windows (11).

Another way to obtain the mean power is through the consideration of the harmonic components of voltages and currents in the frequency domain by using the discrete fourier transform (12). In particular, a fast Fourier transform algorithm is used in order to improve the efficiency. A two-step search for the harmonic peaks is then carried out: (1) the indices of the frequency samples corresponding to the highest spectral peaks provide a rough estimate of the unknown frequencies when the wideband noise superimposed on the signal is below threshold; (2) a more accurate estimate of the harmonic frequencies is carried out to determine the fractional bin frequency (i.e. the harmonic determination up to the frequency resolution); to this aim, several approaches such as zero padding, interpolation techniques, and flat-top window-based techniques can be applied (13).

High-Frequency Power Measurements

High-frequency power measurements can be classified as follows: *low power,* up to 10 mW; *medium power,* from 10 mW to 1 W; and *high power,* greater than 1 W. Meters used for power measurements at radio or microwave frequencies are generally classified as *absorption type* (containing their own load, generally 50 Ω for radio frequencies) and *transmitted* or *through-line type* (where the load is remote from the meter). Independently of the type, power meters are mainly based on thermistors, thermocouples, diodes, or radiation sensors.

Thermal Methods. In this sub-subsection, the main methods based on power dissipation will be examined, namely: (1) thermistor-based, (2) thermocouple-based, and (3) calorimetric.

Thermistor-Based Power Meters. A thermistor is a resistor made up of a combination of highly temperature-sensitive metallic oxides (14). If it is used as a sensor in a power meter, its resistance becomes a function of the temperature rise produced by the applied power.

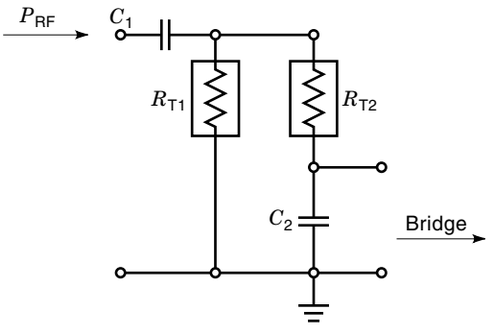

Figure 28. Working principle of the thermistor-based power meter.

The working principle of the thermistor power meter is illustrated in Fig. 28 (15): two thermistors (R_{T1} and R_{T2}) are connected (1) in parallel, for measurand signals appearing at the RF input (P_{RF}) and (2) in series, for the following measuring circuit (e.g. a bridge). The capacitance C_1 prevents the dc power component from flowing to the thermistors; C_2 excludes the RF power from the bridge.

A bridge with a thermistor or a barretter in one arm is called a *bolometer*. Bolometer-based measurements are mainly performed with (1) a manual bolometer with variation of the bias current, (2) a manual bolometer with the substitution method, or (3) a self-balancing bolometer.

The *manual bolometer with a variation of the bias current* is illustrated in Fig. 29. Its working principle consists of two steps. In the first, no RF power is applied to the sensor; the equilibrium is obtained by varying the dc power supply E until the sensor resistance R_B, related to the dc power flowing in it, is equal to R. In this condition let the current I flowing into the circuit be equal to I_1. In the second step, RF power P_{RF} is fed to the sensor; the power increase must be compensated by a dc power decrease, which is performed by lowering the bridge dc supply voltage E; in this case, let I be equal to I_2. Since the power dissipated in the sensor has been maintained constant in both steps, the power P_{RF} can be evalu-

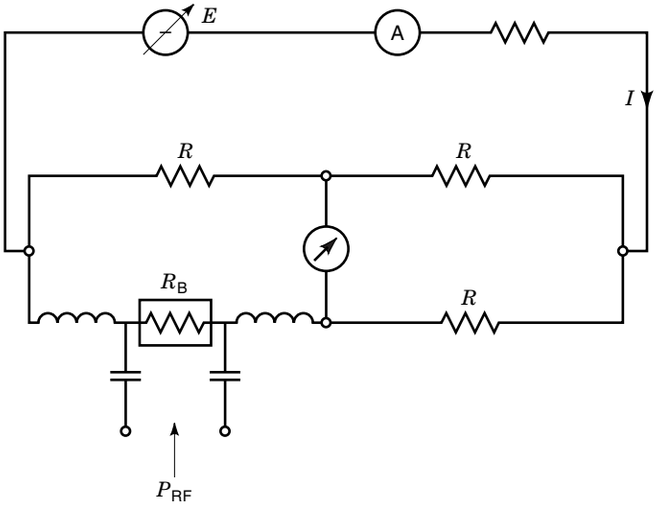

Figure 29. Manual bolometer.

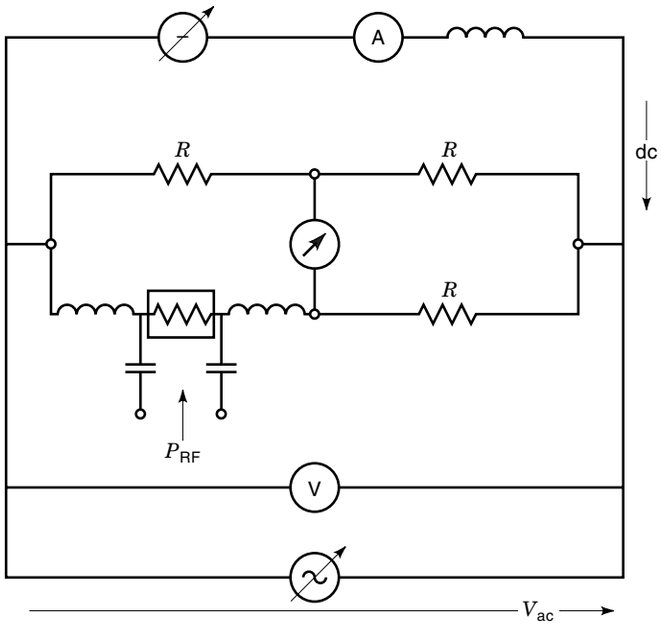

Figure 30. Manual bolometer with substitution method.

ated as

$$P_{RF} = \frac{R}{4}(I_1^2 - I_2^2) \tag{68}$$

The *manual bolometer with the substitution method* (Fig. 30) involves two steps. In the first, both RF power (P_{RF}) and dc power (P_{dc}) are present, and the power (P_d) necessary to bring the bridge to the equilibrium is

$$P_d = P_{dc} + P_{RF} \tag{69}$$

During the second step, P_{RF} is set to zero and an alternating voltage V_{ac} is introduced in parallel with the dc power supply. In this case, the power P_d necessary to balance the bridge,

$$P_d = P_{dc} + P_{ac} \tag{70}$$

is obtained by varying V_{ac}. Since P_d is the same in both cases, the power supplied by the ac generator is equal to

$$P_{RF} = P_{ac} = \frac{V_{ac}^2}{4R} \tag{71}$$

Equation (71) implies that the RF power can be obtained by a voltage measurement.

The *self-balancing bolometer* (Fig. 31) automatically supplies a dc voltage V to balance the voltage variations due to changes in the sensor resistance R_B for an incident power P_{RF}. At equilibrium, R_B is equal to R, and the RF power will then be

$$P_{RF} = \frac{V^2}{4R} \tag{72}$$

As mentioned above, the thermistor resistance depends on the surrounding temperature. This effect is compensated in an instrument based on two self-balancing bridges (15). The RF power is input only to one of these, as shown in Fig. 32.

The equilibrium voltages V_c and V_{RF} feed a chopping and summing circuit, whose output $V_c + V_{RF}$ goes to a voltage-to-time converter. This produces a pulse train V_1, whose width is proportional to $V_c + V_{RF}$. The chopping section also generates a signal with an amplitude proportional to $V_c - V_{RF}$ and a frequency of a few kilohertz, which is further amplified. The signals V_1 and V_2 enter an electronic switch, whose output is measured by a medium-value meter M. This measure is proportional to the RF power, because

$$P_{RF} = \frac{(V_c + V_{RF})(V_c - V_{RF})}{4R} = \frac{V_c^2 - V_{RF}^2}{4R} \tag{73}$$

Owing to the differential structure of the two bolometers, this device is capable of performing RF power measurements independent of the surrounding temperature. In addition, an offset calibration can be carried out when P_{RF} is null and V_c is equal to V_{RF}.

These instruments can range from 10 mW to 1 μW and utilize sensors with frequency bandwidths ranging from 10 kHz to 100 GHz.

Thermocouple-Based Power Meters. Thermocouples (14) can be also used as RF power meters up to frequencies greater than 40 GHz. In this case the resistor is generally a thin-film type.

The sensitivity of a thermocouple can be expressed as the ratio between the dc output amplitude and the input RF power. Typical values are 160 μV/mW for a minimum power of about 1 μW.

The measurement of voltages of some tens of millivolt requires strong amplification, such that the amplifier does not introduce any offset. For this purpose, a chopper microvoltmeter is utilized (16), as shown in the Fig. 33. The thermocouple output voltage V_{dc} is chopped at a frequency of about 100 Hz; the resulting square wave is filtered to its mean value and then input to an ac amplifier to further reduce offset problems. A detector, synchronized to the chopper, and a low-pass filter transform the amplified square-wave voltage to a dc voltage, which is finally measured by a voltmeter.

Calorimetric Method. For high frequencies a substitution technique based on a calorimetric method is utilized (Fig. 34) (17). First, the unknown RF power P_{RF} is sent to the measuring device t, which measures the equilibrium temperature. Then, once the calorimetric fluid has been cooled to its initial temperature, dc power P_{dc} is applied to the device and regulated until the same temperature increase occurs in the same time interval. In this way, a thermal energy equivalence is established between the known P_{dc} and the measurand P_{RF}.

A comparison version of the calorimetric method is also used for lower-frequency power measurements (Fig. 35). One measures the temperature difference ΔT in a cooling fluid be-

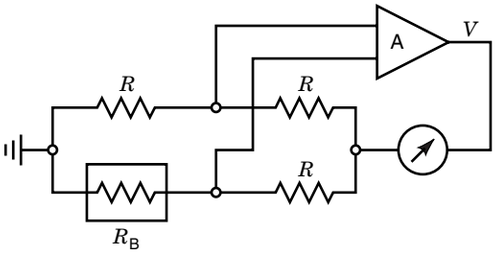

Figure 31. Self-balancing bolometer.

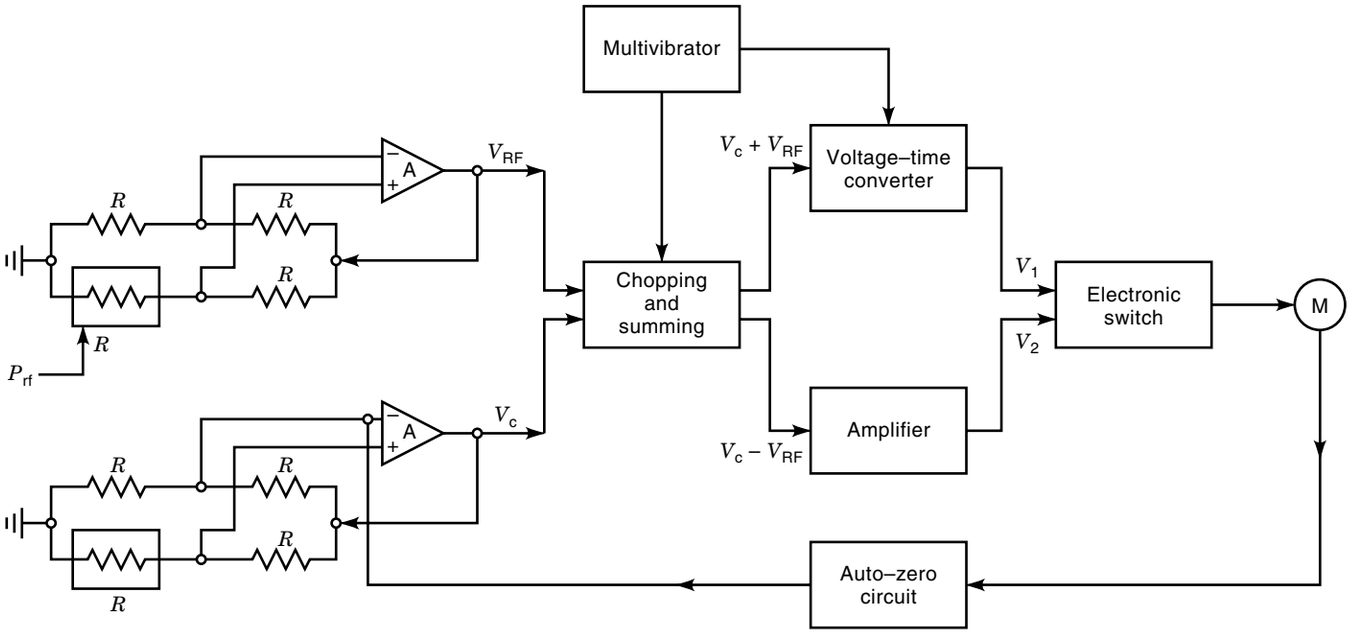

Figure 32. Power meter based on two self-balancing bridges.

tween the input (1) and the output (2) sections of a cooling element where the power P to be measured is dissipated. In this case, the power loss will correspond to P:

$$P = C_p \rho Q \, \Delta T \tag{74}$$

where C_p is the specific heat, ρ the density, and Q the volume flow of the refreshing fluid.

Diode-Sensor-Based Power Measurements. Very sensitive (down to 0.10 nW, −70 dBm) high-frequency (10 MHz to 20 GHz) power measurements are carried out through a diode sensor by means of the circuit in Fig. 36 (18). In particular, by a suitable selection of the components in this circuit, either true-average power measurements or peak power measurements can be performed.

The basic concept underlying *true-average power measurements* exploits the nonlinear (quadratic) region of the characteristic of a low-barrier Schottky diode (nonshaded area in Fig. 37). In this region, the current flowing through the diode is proportional to the square of the applied voltage; thus the diode acts as a quadratic-characteristic sensor.

In the essential circuit of diode sensor-based wattmeters shown in Fig. 36, the measurand v_x, terminated on the matching resistor R_m, is applied to the diode sensor D_s working in its quadratic region in order to produce a corresponding output current i_c in the bypass capacitor C_b. If C_b has been suitably selected, the voltage V_c between its terminals, measured by the voltmeter amplifier V_a, is proportional to the average of i_c, that is, to the average of the squares of instantaneous values of the input signal v_x, and hence to the true-average power.

In the true-average power measurement of nonsinusoidal waveforms having the biggest components at low frequency, as in RF amplitude modulation (AM), the value of C_b must also satisfy another condition. The voltage v_d on the diode must be capable of holding the diode switched on (conducting) even for the smallest values of the signal. Otherwise, in the valleys of the modulation cycle, the high-frequency modulating source is disconnected by the back-biased diode and the measurement is therefore misleading.

On the other hand, for the same signal but for a different selection of the C_b value, the circuit can act as a peak detector for *peak power measurements*. As a matter of fact, the voltage v_c on the bypass capacitor C_b during the peak of the modulation cycle is so large that in the valleys the high-frequency peaks are not capable of switching the diode into conduction; thus these peaks do not contribute to the measured power level.

If higher power levels have to be measured (10 mW to 100 mW), the sensing diode is forced to operate outside the quadratic region, in the linear region (shaded area in Fig. 37). In

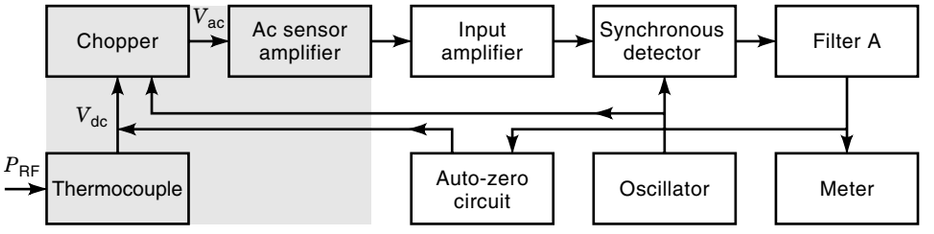

Figure 33. Power meter with thermocouple-based sensor.

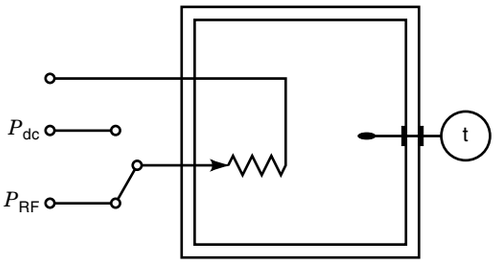

Figure 34. Calorimetric method based on a substitution technique.

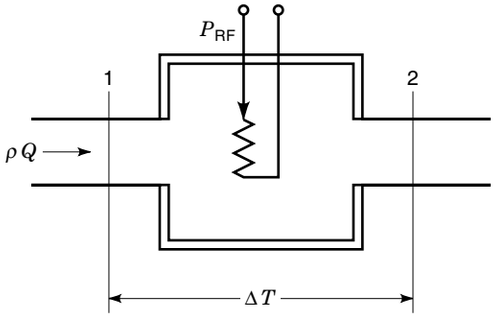

Figure 35. Calorimetric method based on a comparison technique.

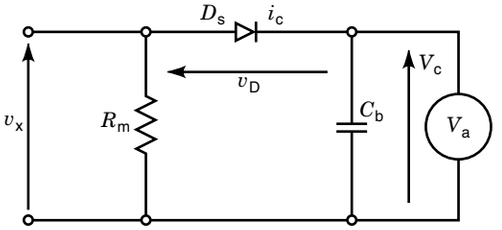

Figure 36. Circuit for diode-sensor-based power measurement.

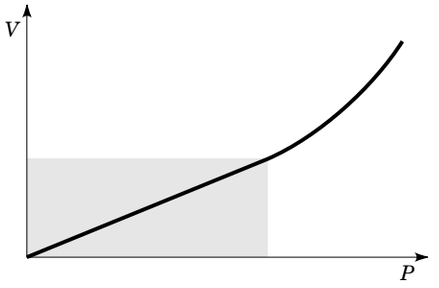

Figure 37. Characteristic of a low-barrier Schottky diode.

this case, the advantage of true-average power measurements for distorted waveforms is lost, and for peak power measurements, since the diode input–output characteristic is nonlinear and the output is quadratic, spectral components different from the fundamental introduce significant measuring errors.

BIBLIOGRAPHY

1. G. Zingales, Measurements on steady-state circuits, in *Methods and Instruments for Electrical Measurements,* (in Italian), Torino: UTET, 1980, Chap. VI.
2. G. Zingales, Power measurements on single-phase ac circuits, in *Methods and Instruments for Electrical Measurements* (in Italian), Torino: UTET, 1980, Chap. VI, Sec. 6.2.
3. G. Korànyi, Measurement of power and energy, in L. Schnell (ed.), *Technology of Electrical Measurements,* Chichester: Wiley, 1993.
4. J. Milmann and C. C. Halkias, *Integrated Electronics: Analog and Digital Circuits and Systems,* New York: McGraw-Hill, 1972.
5. M. L. Sanderson, Power measurement, in *Instrumentation Reference Book,* Butterworths, 1988, Part 3, chap. 1.4.
6. P. S. Filipski, A TDM wattmeter with 0.5 MHz carrier frequency, *IEEE Trans. Instrum. Meas.,* **IM-39**: 15–18, 1990.
7. J. R. Carstens, *Electrical Sensors and Transducers,* Englewood Cliffs, NJ: Prentice-Hall, 1992.
8. Z.-L. Lu, An error estimate for quasi-integer-period sampling and an approach for improving its accuracy, *IEEE Trans. Instrum. Meas.,* **IM-23**: 337–341, 1984.
9. V. Haasz, The error analysis of digital measurements of electrical power, *Measurement,* Vol. 6, No. 4, Oct.–Dec., 1988.
10. P. Arpaia et al., Real-time algorithms for active power measurements on PWM-based electric drives, *IEEE Trans. Instrum. Meas.,* **IM-45**: 462–466, 1996.
11. X. Dai and R. Gretsch, Quasi-synchronous sampling algorithm and its applications, *IEEE Trans. Instrum. Meas.,* **IM-43**: 204–209, 1994.
12. M. Bellanger, *Digital Processing of Signals: Theory and Practice,* Chichester: Wiley, 1984.
13. M. Bertocco, C. Offelli, and D. Petri, Numerical algorithms for power measurements, *Eur. Trans. Electr. Power,* **ETEP 3**: 91–101, 1993.
14. H. N. Norton, Thermometers, in *Handbook of Transducers,* Englewood Cliffs, NJ: Prentice-Hall, 1989, Chap. 19.
15. Anonymous, Thermistor mounts and instrumentation, *Fundamentals of RF and Microwave Power Measurements,* Application Note 64-1, Hewlett Packard, 1978, Chap. II.
16. R. E. Pratt, Power measurements in C. F. Coombs (ed.), *Handbook of Electronic Instruments,* New York: McGraw-Hill, 1995, Secs. 15.1–15.16.
17. F. F. Mazda, High-frequency power measurements, in *Electronic Instruments and Measurement Techniques,* Cambridge, UK: Cambridge University Press, 1987, Chap. VIII, Sec. 8.4.
18. Anonymous, Diode detector power sensors and instrumentation, in *Fundamentals of RF and Microwave Power Measurements,* Application Note 64-1, Hewlett Packard, 1978, Chap. IV.

Reading List

Anonymous, *Fundamentals of RF and Microwave Power Measurements,* Application Note 64-1, Hewlett Packard, 1978. Though not very recent, this is a valid and comprehensive reference for main principles of high-frequency power measurements.

P. Arpaia et al., An expert system for the optimum design of measurement systems, *IEE Proc. A,* **142**: 330–336, 1995. Reports on an

artificial intelligence tool for the automatic design of power-measuring systems.

F. Avallone, C. De Capua, and C. Landi, Measurement station performance optimization for testing on high efficiency variable speed drives, *Proc. IEEE IMTC/96,* Brussels, 1996, pp. 1098–1103. Proposes an analytical model of uncertainty arising from power measurement systems working under highly distorted conditions.

F. Avallone, C. De Capua, and C. Landi, Measurand reconstruction techniques applied to power measurements on high efficiency variable speed drives, *Proc. XIV IMEKO World Congress,* Tampere, 1997. Proposes a technique to improve accuracy of power measurements under highly distorted conditions.

F. Avallone, C. De Capua, and C. Landi, A digital technique based on real-time error compensation for high accuracy power measurement on variable speed drives, *Proc. IEEE IMTC/97,* Ottawa, 1997. Reports on a real-time technique for error compensation of transducers working under highly distorted conditions.

F. Avallone, C. De Capua, and C. Landi, Metrological performance improvement for power measurements on variable speed drives, *Measurement,* vol. 21, no. 1/2, May/June 1997. Shows how to compute the uncertainty of measuring-chain components for power measurements under highly distorted conditions.

G. Bucci, P. D'Innocenzo, and C. Landi, A modular high-speed DSP-based data acquisiton apparatus for on-line quality analysis on power systems under non-sinusoidal conditions, *Proc. 9th IMEKO TC4 Int. Symp.,* Budapest, 1996, pp. 286–289. Gives a strategy of measurement system design for power measurements under non-sinusoidal conditions.

K. K. Clarke and D. T. Hess, A 1000 A / 20 kV / 25 kHz–500 kHz volt–ampere–wattmeter for loads with power factors from 0.001 to 1.00, *IEEE Trans. Instrum. Meas.,* **IM-45**: 142–145, 1996. Provides information on the implementation of an instrument to perform an accurate measurement of currents (1 A to 1000 A), voltages (100 V to 20 kV), and powers (100 W to 20 MW) over the frequency range from 25 kHz to 500 kHz.

J. J. Clarke and J. R. Stockton, Principles and theory of wattmeters operating on the basis of regularly spaced sample pairs, *J. Phys. E. Sci. Instrum.,* **15**: 645–652, 1982. Gives the basis of regularly spaced sample pairs, *J. Phys. E. Sci. Instrum.,* **15**: 645–652, 1982. Gives the basics of synchronous sampling for digital wattmeters.

J. W. Gardner, *Microsensors: Principles and Applications,* Chichester: Wiley, 1994.

S. L. Garverick et al., A programmable mixed-signal ASIC for power metering, *IEEE J. Solid State Circuits,* **26**: 2008–2015, 1991. Reports on a programmable mixed analog–digital integrated circuit based on six first-order sigma–delta ADCs, a bit serial DSP, and a byte-wide static RAM for power metering.

F. K. Harris, The measurement of power, in *Electrical mesurements,* Huntington, NY: Krieger, 1975, Chap. XI. A clear reference for line-frequency power measurements.

J. K. Kolanko, Accurate measurement of power, energy, and true rms voltage using synchronous counting, *IEEE Trans. Instrum. Meas.,* **IM-42**: 752–754, 1993. Provides information on the implementation of a synchronous dual-slope wattmeter.

F. F. Mazda, Pulse power measurement, in *Electronic Instruments and Measurement Techniques,* Cambridge, UK: Cambridge University Press, 1987, Chap. VIII, Sec. 8.5.

J. C. Montano et al., DSP-based algorithm for electric power measurement, *IEE Proc. A,* **140**: 485–490, 1993. Descries a Goertzel FFT-based algorithm to compute power under nonsinusoidal conditions.

H. N. Norton, Radiation pyrometers, in *Handbook of Transducers,* Englewood Cliffs, NJ: Prentice-Hall, 1989, Chap. 20.

T. S. Rathore, Theorems on power, mean and rms values of uniformly sampled periodic signals, *IEE Proc. A,* **131**: 598–600, 1984. Provides fundamental theorems for effective synchronous sampling wattmeters.

G. N. Stenbakken, A wideband sampling wattmeter, *IEEE Trans. Power Appar. Syst.,* **PAS-103**: 2919–2925, 1984. Gives the basics of asynchronous-sampling-based wattmeters and criteria for computing uncertainty in the time domain.

GIOVANNI BUCCI
CARMINE LANDI
University of Aquila
CLAUDIO DE CAPUA
Federico II University of Naples

POWER MEASUREMENT.

See VOLT-AMPERE METERS.